



## [18]Annulene put into a new perspective†‡

Cite this: *Chem. Commun.*, 2016, 52, 4710Dominik Lungerich,<sup>a</sup> Alexey V. Nizovtsev,<sup>b</sup> Frank W. Heinemann,<sup>b</sup> Frank Hampel,<sup>a</sup> Karsten Meyer,<sup>b</sup> George Majetich,<sup>c</sup> Paul v. R. Schleyer<sup>c</sup> and Norbert Jux<sup>\*a</sup>Received 11th February 2016,  
Accepted 2nd March 2016

DOI: 10.1039/c6cc01309k

www.rsc.org/chemcomm

**New insights into [18]annulene were gained by looking more closely at its X-ray structure, revealing a close face-to-face stacking of 3.16 Å in a herringbone-like crystal packing. Hexadehydro[18]annulene was co-crystallized in a benzene matrix, demonstrating the stabilizing role of intercalated solvent molecules in solid annulenes.**

The story of [18]annulene **1** – its structural elucidation and its aromaticity – is probably one of the most controversially discussed issues in the field of physical organic chemistry, even though it represents one of the classic molecules found in virtually every organic and spectroscopy textbook.<sup>1,2</sup> Originally, with its 18 $\pi$  electrons, its preparation served the understanding of larger aromatic compounds<sup>3,4</sup> that follow Hückels  $(4n + 2)\pi$  rule and the distinction, up to which ring size aromaticity has an effect on bond length alternation and a stabilizing effect on the molecule.<sup>5–7</sup> Down to the present day, **1** has set off an avalanche of publications mostly theoretical in nature concerning *e.g.*, the re-evaluation of its aromaticity,<sup>8</sup> or as a model compound for the ring-current in porphyrin **2** and related tetrapyrroles.<sup>9</sup> However, as for experimental research, **1** has withered away from the current literature, most likely due to its tendency to decompose, accompanied by unattractive overall yields of 0.4 to 0.6%, respectively.<sup>10,11</sup>

Accompanied by a modern and improved synthesis, we discuss here [18]annulene **1** for the first time from a materials chemical perspective.<sup>12</sup> We re-investigated its brown crystals,

grown from diethyl ether and methanol at  $-20\text{ }^{\circ}\text{C}$ , which were elucidated by means of X-ray diffraction. **1** crystallizes in the space group  $P2_1/n$  as shown in Fig. 1c. We found essentially the same structural characteristics as already described in 1995.<sup>4</sup> Taking a closer look at the larger crystal packing, presented in Fig. 1a and b, we were exhilarated by its similarity to the herringbone packing of pentacene **3a**.<sup>13</sup> However, a critical difference between **3a** and **1** is given by the very intimate face-to-face distance of only 3.16 Å between the respective  $\pi$ -surfaces (see Fig. 2a and c) in **1**. Comparing the distances between individual graphene sheets in graphite – 3.35 Å,<sup>14</sup> the layers in crystals of TIPS-pentacene **3b** – 3.43 Å,<sup>15</sup> or in coronene **4** – 3.46 Å,<sup>16</sup> the reduced face-to-face association of up to 0.4 Å in **1** is significant. The discrepancy between layers of **1** and **4** – which share the same outer carbon skeleton – can be explained by the “annulene-hole”. The van der Waals radii of the inner C–H bonds in **1** are around 0.4 Å smaller in size than those of the respective C–C bonds in **4**, resulting in closer  $\pi$ – $\pi$  stacks. Thus, the repulsive vdW forces of the outer carbon framework of **1** remain essentially the same as in **4**. However, the slipped stacking of **1** that allows overlap in the “annulene-hole” region, which is non-existent in **4**, is most likely responsible for this closer interaction.<sup>4</sup> Hence, directly overlapping stacks of **1** would probably result in comparable stacking distances as in coronene **4**. The exact nature of this effect remains not fully understood yet. § Fig. 2b shows the HOMO and the LUMO of **1**. Both MOs are distributed equally over the cyclic molecule, assuming a sufficient electronic communication in the solid state. The C–C edge-to-face distance is 3.52 Å and the molecules stand at an angle of  $82.4^{\circ}$  to each other, respectively. We investigated thin-films of **1** by means of solid state absorption spectroscopy. Therefore, we drop-cast **1** from a  $10^{-5}$  M  $\text{CH}_2\text{Cl}_2$  solution, which was evaporated under a continuous  $\text{N}_2$ -flow. As shown in Fig. 3, **1** shows distinct absorption maxima at 375 nm ( $300\,000\text{ M}^{-1}\text{ cm}^{-1}$ ) and at 454 nm ( $25\,000\text{ M}^{-1}\text{ cm}^{-1}$ ) in solution. The optical bandgap  $E_g$  was estimated from solution ( $\text{CH}_2\text{Cl}_2$ ), based on the intercept of a tangent applied to the lower edge of the longest wavelength absorption and the  $x$ -axis,

<sup>a</sup> Department Chemie und Pharmazie & Interdisciplinary Center for Molecular Materials (ICMM), Organic Chemistry II, Friedrich-Alexander-Universität Erlangen-Nürnberg, Henkestraße 42, 91054, Erlangen, Germany.  
E-mail: norbert.jux@fau.de

<sup>b</sup> Department Chemie und Pharmazie, Inorganic Chemistry, Friedrich-Alexander-Universität Erlangen-Nürnberg, Egerlandstraße 1, 91058, Erlangen, Germany

<sup>c</sup> Department of Chemistry, University of Georgia, 140 Cedar St, Athens, GA 30602, USA

† Dedicated to our friend and mentor, Paul von Ragué Schleyer.

‡ Electronic supplementary information (ESI) available: Experimental procedures, spectra, and X-ray data. CCDC 1452788 (**1**) and 1452902 (**5**). For ESI and crystallographic data in CIF or other electronic format see DOI: 10.1039/c6cc01309k



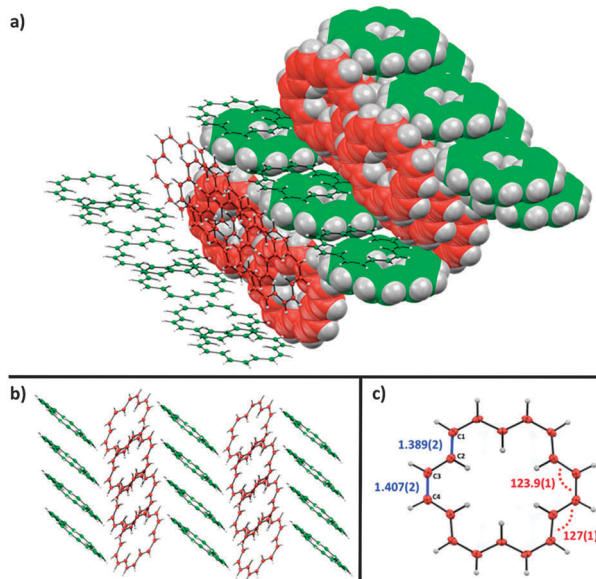
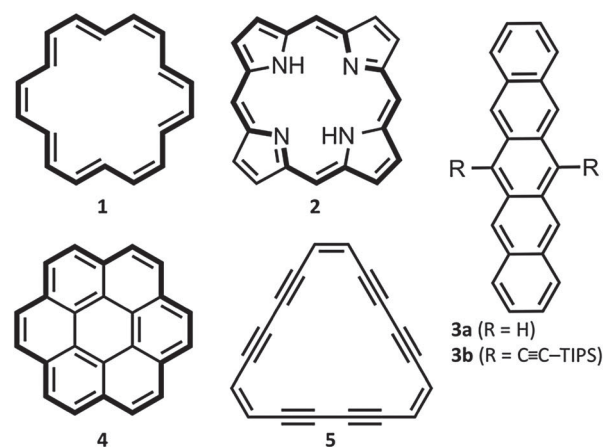


**Fig. 1** X-ray structure analysis of **1**: (a) crystal packing depicted as space-filling model and as ORTEP model; (b) side view of herringbone pattern; (c) crystal structure, showing averaged bond lengths indicated in blue and averaged bond angles depicted in red; ORTEP models are depicted as 50% thermal ellipsoids.

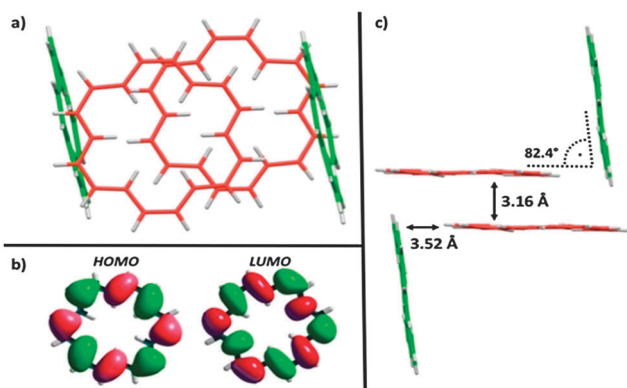


**Fig. 2** Analysis of **1**: (a) top-view of molecular overlap in crystal packing; (b) DFT calculation of HOMO and LUMO at the B3LYP/6-311G\* level of theory; (c) side-view of crystal packing.

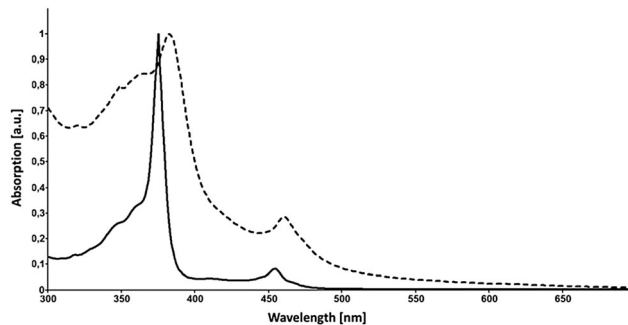


**Fig. 3** Absorption spectra of **1** in solution (CH<sub>2</sub>Cl<sub>2</sub>, solid line) and in the solid state (dashed line).

indicating an energy gap of 2.64 eV (469 nm). The solid state spectrum of **1** (dashed line in Fig. 3) shows broadened absorption characteristics and a peculiar red-shift of 7 and 6 nm to 382 and 460 nm, respectively. The bathochromic shift indicates close  $\pi$ -stacks, similar to those depicted in the crystal packing. Even though there is still much controversy regarding the electronic transport in organic materials, it remains irrefutable that interlocked layers in herringbone-like structured van der Waals crystals are prone to higher field-effect mobilities.<sup>17</sup> Nonetheless, we relinquished to perform actual device experiments with **1**, since it is clearly not a realistic candidate. Its thermal instability and its tendency to decompose rapidly are probably the most significant arguments not to study its device applicability.<sup>17</sup> However, functionalized non-benzenoid derivatives of **1** that make use of the “annulene-hole” in order to get into close face-to-face contact, might become an important strategy for the design of organic materials.

A pivotal role in the synthesis of **1** is played by the triangular hexadehydro[18]annulene **5**. Even though it has been reported nearly 50 years ago,<sup>18,19</sup> we were quite surprised not to find any discussion about its crystal structure and crystal packing in the literature.<sup>20</sup> This might be due to its well-known instability in the solid state and even explosive decomposition above 85 °C.<sup>18,20</sup> We grew stable amber single crystals of **5** from a slowly evaporated mixture of benzene and diethyl ether at -20 °C. Although **5** represents an 18 $\pi$  aromatic compound, the structure shows clearly bond length alternation of localized single-, double-, and triple bonds.<sup>21</sup> Bond lengths and - angles are shown in Fig. 4a. **5** crystallizes in the tetragonal space group *I41/acd* and adapts an almost planar geometry. It shows a parallel arranged packing, in which benzene molecules are co-crystallized in an array of small nano-channels, formed by **5** (compare Fig. 4b-d). Unlike in crystals of **1**, the layer distance is increased to 3.60 Å and consequently exceeds even the values reached by **3b** and **4**. This range jump is most likely explained by the intercalated benzene molecules that serve as a barrier for structural decay. The most likely decomposition mechanism in dehydroannulenes represents the [2+2] alkyne-alkyne polymerization.<sup>2,22</sup> However, the symmetrically arranged molecules in the co-crystallized benzene framework are rather badly positioned for [2+2] polymerizations. Nonetheless, under freeze-drying conditions – the slow removal of benzene at low temperatures – **5** shows a rapid



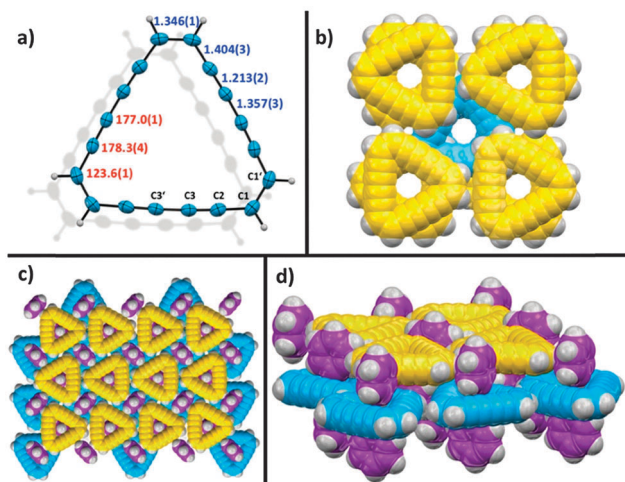
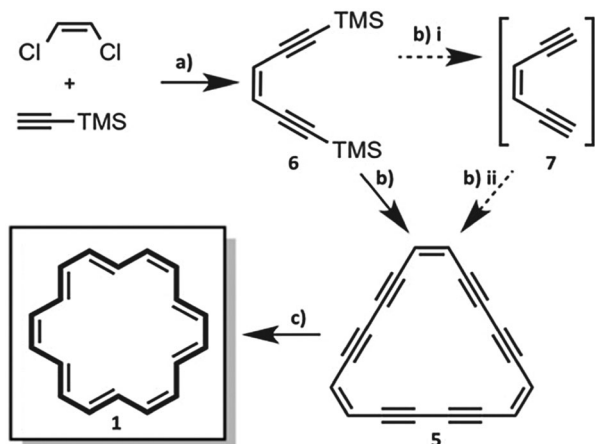


Fig. 4 X-ray structure analysis of **5**: (a) crystal structure, showing averaged bond lengths indicated in blue and averaged bond angles depicted in red; ORTEP models are depicted as 50% thermal ellipsoids (b) top-view on crystal packing depicted as space-filling model, showing the nano-channel array; benzene molecules are omitted for clarity; (c) top-view on crystal packing depicted as space-filling model; (d) perspective side-view on crystal packing; benzene molecules are depicted in purple for clarity.

decomposition to black amorphous carbon within a few hours, underlining the importance of intercalated solvent molecules in highly unsaturated hydrocarbons.

**1** and **5** were synthesized by a revisited and feasible protocol that takes advantage of modern laboratorial techniques (Scheme 1). We coupled commercially available *cis*-1,2-dichloroethene and TMS-acetylene with 4% Pd(PPh<sub>3</sub>)<sub>2</sub>Cl<sub>2</sub> and 2% CuI in *n*-butylamine and benzene and obtained **6** in 90% yield.<sup>23</sup> **6** was deprotected with tetrabutylammonium fluoride (TBAF) in THF at 0 °C, followed by a subsequent oxidative cyclization under modified Eglinton conditions, indicating excess of copper(II) acetate in pyridine at room temperature.<sup>24</sup> At an estimated molarity of 45 mM solution of hexenediynes **7** in the pyridine/Cu mixture,



Scheme 1 Improved synthesis of **1** and **5**: (a) 2% Pd(PPh<sub>3</sub>)<sub>2</sub>Cl<sub>2</sub>, 4% CuI in benzene/*n*-butylamine, r.t. (90%); (b) (i) 1 M TBAF in THF, 0 °C, (ii) excess Cu(OAc)<sub>2</sub>·H<sub>2</sub>O in pyridine, r.t. (24%); (c) 5% Pd/CaCO<sub>3</sub>/Pb, quinoline, 1 atm H<sub>2</sub> in benzene, r.t. (20%).

yields of up to 24% of **5** were obtained. As reported earlier, the selective reduction of **5** to **1** remains difficult, since [18]annulene **1** is hydrogenated faster than hexadehydro[18]-annulene **5**.<sup>3,10</sup> Hydrogenation of **5** with 5% Pd/CaCO<sub>3</sub>/Pb (Lindlar catalyst) that was additionally poisoned with quinoline under 1 atm H<sub>2</sub> gas was terminated upon complete consumption of the starting material (typically after one hour). **1** was obtained in an average yield of 20%. The overall yield of 4% over three steps remains low; however, it represents the highest reported yield of **1**.<sup>10,11</sup> Lastly, regarding the stability of **1** and **5**, we found a very convenient way to store these annulenes, without any observed decomposition for several months. Therefore, a dilute frozen solution of **1** or **5** in benzene at –20 °C served very well as a protecting matrix.

To summarize, we improved the synthesis of [18]annulene **1** in a three-step protocol with yields exceeding reported values by a factor of ten. With the first X-ray structure of hexadehydro[18]-annulene **5**, co-crystallized in a benzene matrix, we were able to discuss the role of intercalated solvent residues as a protector towards decomposition to amorphous carbon. The crystal structure analysis of **1** revealed a herringbone-like stacking pattern, with face-to-face distances as low as 3.16 Å, thus undercutting the  $\pi$ - $\pi$ -contacts of pentacene and coronene by a value of 0.4 Å. This distance discrepancy is attributed to the inner C–H bonds, the “annulene-hole”. By solid state UV/vis experiments, we observed a red-shift of the absorption characteristics that are most likely caused by stacking phenomena. We believe that engineering the periphery of annulenes (excluding benzannelation) will lead to unique properties, concerning material chemical performances and might establish a new class in organic electronics. Derivatization of **1** and device experiments are currently under investigation.

## Notes and references

§ We are currently performing a theoretical study on this topic which will be published separately.

¶ M. J. Frisch, G. W. Trucks, H. B. Schlegel, G. E. Scuseria, M. A. Robb, J. R. Cheeseman, J. A. Montgomery, Jr., T. Vreven, K. N. Kudin, J. C. Burant, J. M. Millam, S. S. Iyengar, J. Tomasi, V. Barone, B. Mennucci, M. Cossi, G. Scalmani, N. Rega, G. A. Petersson, H. Nakatsuji, M. Hada, M. Ehara, K. Toyota, R. Fukuda, J. Hasegawa, M. Ishida, T. Nakajima, Y. Honda, O. Kitao, H. Nakai, M. Klene, X. Li, J. E. Knox, H. P. Hratchian, J. B. Cross, V. Bakken, C. Adamo, J. Jaramillo, R. Gomperts, R. E. Stratmann, O. Yazyev, A. J. Austin, R. Cammi, C. Pomelli, J. W. Ochterski, P. Y. Ayala, K. Morokuma, G. A. Voth, P. Salvador, J. J. Dannenberg, V. G. Zakrzewski, S. Dapprich, A. D. Daniels, M. C. Strain, O. Farkas, D. K. Malick, A. D. Rabuck, K. Raghavachari, J. B. Foresman, J. V. Ortiz, Q. Cui, A. G. Baboul, S. Clifford, J. Cioslowski, B. B. Stefanov, G. Liu, A. Liashenko, P. Piskorz, I. Komaromi, R. L. Martin, D. J. Fox, T. Keith, M. A. Al-Laham, C. Y. Peng, A. Nanayakkara, M. Challacombe, P. M. W. Gill, B. Johnson, W. Chen, M. W. Wong, C. Gonzalez and J. A. Pople, *Gaussian 03, Revision C.02*, Gaussian, Inc., Wallingford CT, 2004.

- 1 F. Sondheimer and R. Wolovsky, *Tetrahedron Lett.*, 1959, **1**, 3–6.
- 2 E. L. Spitler, C. A. Johnson and M. M. Haley, *Chem. Rev.*, 2006, **106**, 5344–5386.
- 3 F. Sondheimer, R. Wolovsky and Y. Amiel, *J. Am. Chem. Soc.*, 1962, **84**, 274–284.
- 4 S. Gorter, E. Rutten-Keulemans, M. Krever, C. Romers and D. W. J. Cruickshank, *Acta Crystallogr., Sect. B: Struct. Sci.*, 1995, **51**, 1036–1045.
- 5 J. F. M. Oth, J.-C. Bünzli and Y. de J. Zélicourt, *Helv. Chim. Acta*, 1974, **57**, 2276–2288.
- 6 K. Stöckel, P. J. Garratt and F. Sondheimer, *J. Am. Chem. Soc.*, 1972, **94**, 8644–8645.



- 7 S. C. A. H. Pierrefixe and F. M. Bickelhaupt, *J. Phys. Chem. A*, 2008, **112**, 12816–12822.
- 8 C. S. Wannere, K. W. Sattelmeyer, H. F. Schaefer and P. V. R. Schleyer, *Angew. Chem., Int. Ed.*, 2004, **43**, 4200–4206; C. S. Wannere and P. V. R. Schleyer, *Org. Lett.*, 2003, **5**, 865–868; C. H. Choi, M. Kertesz and A. Karpfen, *J. Am. Chem. Soc.*, 1997, **119**, 11994–11995; K. Jug and E. Fasold, *J. Am. Chem. Soc.*, 1987, **109**, 2263–2265.
- 9 T. D. Lash, A. Sun, T. Chaney and D. T. Richter, *J. Org. Chem.*, 1998, **63**, 9076–9088; T. D. Lash, S. A. Jones and G. M. Ferrence, *J. Am. Chem. Soc.*, 2010, **132**, 12786–12787; H. Fliegl and D. Sundholm, *J. Org. Chem.*, 2012, **77**, 3408–3414; J. I. Wu, I. Fernández and P. V. R. Schleyer, *J. Am. Chem. Soc.*, 2013, **135**, 315–321; M. K. Cyrański, T. M. Krygowski, M. Wisiorowski, N. J. R. van Eikema Hommes and P. V. R. Schleyer, *Angew. Chem., Int. Ed.*, 1998, **37**, 177–180.
- 10 H. P. Figeys and M. Gelbcke, *Tetrahedron Lett.*, 1970, 5139–5142.
- 11 K. Stöckel and F. Sondheimer, *Org. Synth.*, 1974, **54**, 1.
- 12 M. Iyoda, J. Yamakawa and M. J. Rahman, *Angew. Chem., Int. Ed.*, 2011, **50**, 10522–10553.
- 13 C. C. Mattheus, A. B. Dros, J. Baas, A. Meetsma, J. L. de Boer and T. T. Palstra, *Acta Crystallogr., Sect. C: Cryst. Struct. Commun.*, 2001, **57**, 939–941.
- 14 N. Wiberg, *Lehrbuch der Anorganischen Chemie*, Walter de Gruyter & Co., 2007, pp. 864–865.
- 15 J. E. Anthony, J. S. Brooks, D. L. Eaton and S. R. Parkin, *J. Am. Chem. Soc.*, 2001, **123**, 9482–9483.
- 16 J. Monteath Robertson and J. G. White, *J. Chem. Soc.*, 1945, 607–617.
- 17 H. Klauk, *Organic electronics, Materials, Manufacturing, and Applications*, Wiley-VCH Verlag GmbH, 2006, pp. 39–41.
- 18 W. H. Okamura and F. Sondheimer, *J. Am. Chem. Soc.*, 1967, **89**, 5991–5992.
- 19 F. Sondheimer, Y. Amiel and Y. Gaoni, *J. Am. Chem. Soc.*, 1962, **84**, 270–274.
- 20 M. Suzuki, A. Comito, S. I. Khan and Y. Rubin, *Org. Lett.*, 2010, **12**, 2346–2349.
- 21 J. Juselius and D. Sundholm, *Phys. Chem. Chem. Phys.*, 2001, **3**, 2433–2437.
- 22 Q. Zhou, P. J. Carroll and T. M. Swager, *J. Org. Chem.*, 1994, **59**, 1294–1301; M. Laskoski, W. Steffen, J. G. M. Morton, M. D. Smith and U. H. F. Bunz, *J. Am. Chem. Soc.*, 2002, **124**, 13814–13818.
- 23 D. Chemin and G. Linstrumelle, *Tetrahedron*, 1994, **50**, 5335–5344.
- 24 G. Eglinton and A. R. Galbraith, *Chemistry and Industry*, 1956, p. 737; F. Sondheimer, Y. Amiel and R. Wolovsky, *J. Am. Chem. Soc.*, 1959, **81**, 4600–4606.

